

ORNL/TM--12248

DE93 007788

Fusion Energy Division

**AN OUTGOING ENERGY FLUX BOUNDARY  
CONDITION FOR FINITE DIFFERENCE  
ICRF ANTENNA MODELS**

D. B. Batchelor  
M. D. Carter

Date published: November 1992

Prepared by  
OAK RIDGE NATIONAL LABORATORY  
Oak Ridge, Tennessee 37831-6285  
managed by  
MARTIN MARIETTA ENERGY SYSTEMS, INC.  
for the  
U.S. DEPARTMENT OF ENERGY  
under contract DE-AC05-84OR21400

**MASTER**

DISTRIBUTION OF THIS DOCUMENT IS UNLIMITED 

## CONTENTS

ABSTRACT . . . . .	v
1. INTRODUCTION . . . . .	1
2. DERIVATION OF THE BOUNDARY CONDITION . . . . .	2
3. APPLICATION TO A SIMPLE 2D PROBLEM . . . . .	8
4. RESULTS OF 2D CALCULATION AND DISCUSSION . . . . .	11
ACKNOWLEDGMENT . . . . .	15
REFERENCES . . . . .	16

## ABSTRACT

For antennas at the ion cyclotron range of frequencies (ICRF) modeling in vacuum can now be carried out to a high level of detail such that shaping of the current straps, isolating septa, and discrete Faraday shield structures can be included. An efficient approach would be to solve for the fields in the vacuum region near the antenna in three dimensions by finite methods and to match this solution at the plasma-vacuum interface to a solution obtained in the plasma region in one dimension by Fourier methods. This approach has been difficult to carry out because boundary conditions must be imposed at the edge of the finite difference grid on a point-by-point basis, whereas the condition for outgoing energy flux into the plasma is known only in terms of the Fourier transform of the plasma fields. A technique is presented by which a boundary condition can be imposed on the computational grid of a three-dimensional finite difference, or finite element, code by constraining the discrete Fourier transform of the fields at the boundary points to satisfy an outgoing energy flux condition appropriate for the plasma. The boundary condition at a specific grid point appears as a coupling to other grid points on the boundary, with weighting determined by a kernel calculated from the plasma surface impedance matrix for the various plasma Fourier modes. This boundary condition has been implemented in a finite difference solution of a simple problem in two dimensions, which can also be solved directly by Fourier transformation. Results are presented, and it is shown that the proposed boundary condition does enforce outgoing energy flux and yields the same solution as is obtained by Fourier methods.

## 1. INTRODUCTION

Ion cyclotron range of frequencies (ICRF) antennas are complicated, three-dimensional (3D) structures whose performance can be affected by details of the geometry. The modeling of such antennas in vacuum is now sophisticated enough that minute details of the structure can be treated, including curved current straps, isolating septa, and discrete Faraday shield structures. This is typically done using finite difference or finite element computer codes (KRESS *et al.*, 1991; RYAN *et al.*, 1990). The presence of the plasma near the antenna is a critical feature, since induced currents in the antenna structure influence the spectrum of power radiated into the plasma. In turn, calculations with two-dimensional (2D) models (BATCHELOR *et al.*, 1992) have shown that radio-frequency (RF) plasma currents induce their own image currents in the antenna, which can cause significant discrepancies between the loading and radiated spectrum calculated from self-consistent antenna/wall currents and the values predicted from vacuum measurements and calculations. It is generally not computationally feasible to include the plasma region in a 3D finite difference code because of the large plasma volume relative to the wavelength and the complexity of the plasma constitutive relation. In any case, from the antenna coupling standpoint, the plasma is essentially one-dimensional (only radial variation is important), so that 3D calculation of the RF fields inside the plasma by finite methods is an unnecessary computational burden.

A logical approach would be to solve for the fields in three dimensions near the antenna and to match this solution to a plasma solution which, because of the lower dimensionality of the plasma, can be obtained by Fourier methods. It has been difficult to carry out such a program because boundary conditions must be imposed at the edge of the finite difference grid on a point-by-point basis, whereas the condition for outgoing energy flux into the plasma is known only in terms of the Fourier transform of the fields in the plasma. We have now developed a technique by which a boundary condition can be imposed on the computational grid by constraining the discrete Fourier transform of the fields at the boundary points to satisfy an outgoing energy flux condition appropriate for the plasma. The boundary condition at a specific grid point appears as a coupling to other grid points on the boundary, with weighting determined by

a kernel calculated from the plasma surface impedance matrix for the various Fourier modes.

In Section 2 we give a derivation of the method for coupling a 3D finite difference solution in a vacuum region to Fourier representations of the field solution in a semi-infinite slab plasma. In order to verify that this scheme does indeed impose the expected boundary condition, we have implemented a 2D finite difference model and applied it to the case of a simple current strap over a conducting ground plane, radiating into a slab plasma—a problem for which a solution is also available using Fourier methods. Section 3 describes the 2D model. Section 4 gives results of the finite difference model and compares them to the solution in terms of Fourier transforms.

## 2. DERIVATION OF THE BOUNDARY CONDITION

We consider the situation illustrated in Fig. 1. The region  $x < 0$  is vacuum containing an arbitrary 3D antenna structure. The computational domain extends over poloidal length  $0 \leq y \leq a$  and toroidal length  $0 \leq z \leq b$ . We assume the fields to be periodic in the  $y$  (poloidal) and  $z$  (toroidal) directions. It is not necessary that  $a$  extend to  $2\pi R_{\min}$  or that  $b$  extend to  $2\pi R_T$  ( $R_{\min}$  = minor radius,  $R_T$  = major radius) in order to adequately model the antenna in cases for which the fields fall rapidly to zero with distance from the antenna. A magnetized plasma exists in the region  $x \geq 0$ , which is uniform in the poloidal and toroidal directions,  $n_s(\mathbf{x}) = n_s(x)$ ,  $\mathbf{B}_0(x) = B_0(x) \hat{\mathbf{z}}$ , where  $n_s$  is the particle density of species  $s$  and  $\mathbf{B}_0$  is the equilibrium magnetic field.

The field in the vacuum region is presumed to be obtained from a finite difference or finite element solution of Maxwell's equations in three dimensions,

$$\begin{aligned} \nabla \times \mathbf{E} &= i\omega \mathbf{B} , \\ \nabla \times \mathbf{B} &= -i\omega \mathbf{E} - i\omega \mu_0 \mathbf{J}_{\text{ext}} , \end{aligned} \tag{1}$$

subject to appropriate boundary conditions on the metal structure, periodic boundary conditions at  $z = 0, b$  and at  $y = 0, a$ , and conditions of outgoing energy flow at the plasma-vacuum interface,  $x = 0$ . The task at hand then is to impose such outgoing energy boundary conditions on the finite difference solution in terms of the Fourier representation of the field in the plasma region.

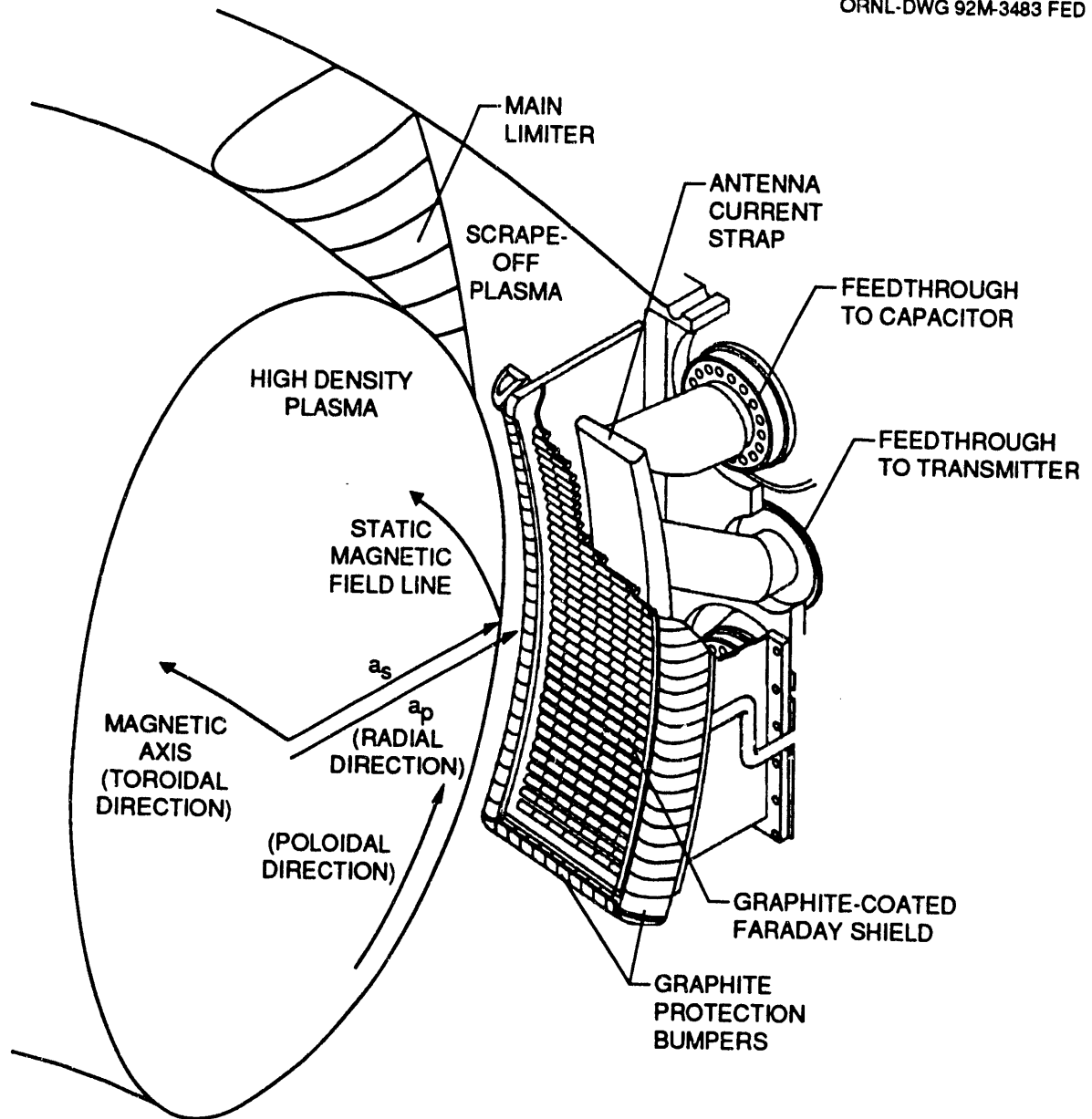


Fig. 1. Geometry of 3D antenna structure radiating into slab plasma having variation only in the  $x$ -direction.

This boundary condition involves imposing the proper linear relation between the wave electric field and magnetic field (or equivalently between the wave electric field and its derivatives) at the edge of the computational grid. Precisely which field components are needed depends on details of the numerical implementation. For concreteness we assume that  $\mathbf{B}_T$ , the tangential components of  $\mathbf{B}$ , are to be expressed in terms of  $\mathbf{E}_T$ , the tangential components of  $\mathbf{E}$ .

In the plasma region the fields satisfy a wave equation of the form

$$\begin{aligned}\nabla \times \mathbf{E} &= i\omega \mathbf{B} , \\ \nabla \times \mathbf{B} &= -i\omega \mathbf{E} - i\omega\mu_0 \mathbf{J}_P ,\end{aligned}\tag{2}$$

where  $\mathbf{J}_P$  is the wave-induced plasma current. Typically we assume  $\mathbf{J}_P$  to be of the form  $\mathbf{J}_P = \Sigma \cdot \mathbf{E}$ , where  $\Sigma$  is the cold or warm plasma conductivity tensor. Nothing in the formulation, however, prevents  $\mathbf{J}_P$  from being a more general operator, such as an integral operator that requires no small Larmor radius expansion. In view of the uniformity of the plasma in the  $y$ - and  $z$ -directions,  $\mathbf{E}$  and  $\mathbf{B}$  can be expanded in a Fourier series,

$$\mathbf{E}(\mathbf{x}) = \sum_{mn\sigma} A_\sigma^{mn} \mathbf{E}_\sigma^{mn}(x) e^{2\pi i(my/a + nz/b)} ,\tag{3}$$

where  $\sigma = 1, 2$  indicates the two independent polarizations at the plasma edge. Equation (2) then becomes a set of ordinary differential equations for each value of  $m, n, \sigma$ . For given  $m, n$  there are in general several modes that propagate in the plasma, for example fast and slow cyclotron waves and, in a warm plasma, Bernstein waves. When a warm plasma is treated the temperature profile is taken to go smoothly to zero at the plasma boundary, so that the solutions are determined uniquely from the tangential components of  $\mathbf{E}$  (or  $\mathbf{B}$ ) at the plasma boundary. Bernstein waves, if present, are excited by the fields penetrating into the plasma. The zero temperature boundary condition then ensures that Bernstein waves propagating in the direction of negative  $x$  are totally reflected inside the plasma.

Equations (2) are solved for each  $m, n, \sigma$ , imposing on each solution a boundary condition of outgoing energy flux at large  $x$  and an initial magnetic field polarization at  $x = 0$ ,

$$\mathbf{b}_\sigma^{mn} \equiv \mathbf{B}_T(x=0)^{mn} = b_{y\sigma}^{mn} \hat{\mathbf{y}} + b_{z\sigma}^{mn} \hat{\mathbf{z}} .$$

A convenient choice for the polarization eigenvectors is  $(b_{y\sigma}^{mn} = 1, b_{z\sigma}^{mn} = 0)$  for  $\sigma = 1$  (slow wave excitation),  $(b_{y\sigma}^{mn} = 0, b_{z\sigma}^{mn} = 1)$  for  $\sigma = 2$  (fast wave excitation), although such a choice is not required. By this process we obtain the plasma eigenfunctions  $\mathbf{E}_\sigma^{mn}(x)$  of Eq. (3) with the  $A_\sigma^{mn}$  representing coefficients to be determined.

Evaluating  $\mathbf{E}_\sigma^{mn}(x = 0)$ , we can construct an effective plasma surface impedance matrix  $\mathbf{Z}^{mn}$  which expresses for the  $m, n$  Fourier mode the tangential electric field at the plasma-vacuum boundary in terms of the tangential magnetic field,  $\mathbf{E}_\mathbf{T}^{mn} = \mathbf{Z}^{mn} \cdot \mathbf{B}_\mathbf{T}^{mn}$ . Introducing the 2D electric field polarization eigenvectors,

$$\mathbf{e}_\sigma^{mn} \equiv \mathbf{E}_\mathbf{T}_\sigma^{mn}(x = 0) = E_{y\sigma}^{mn} \hat{\mathbf{y}} + E_{z\sigma}^{mn} \hat{\mathbf{z}} ,$$

we have, in particular,

$$\mathbf{e}_\sigma^{mn} = \mathbf{Z}^{mn} \cdot \mathbf{b}_\sigma^{mn} ,$$

so the tangential part of Eq. (3), evaluated at  $x = 0$ , can be expressed as

$$\mathbf{E}_\mathbf{T}(0, y, z) = \sum_{mn\sigma} A_\sigma^{mn} \mathbf{e}_\sigma^{mn} e^{2\pi i(my/a + nz/b)} = \sum_{mn\sigma} A_\sigma^{mn} \mathbf{Z}^{mn} \cdot \mathbf{b}_\sigma^{mn} e^{2\pi i(my/a + nz/b)} , \quad (4)$$

whereas

$$\mathbf{B}_\mathbf{T}(0, y, z) = \sum_{mn\sigma} A_\sigma^{mn} \mathbf{b}_\sigma^{mn} e^{2\pi i(my/a + nz/b)} . \quad (5)$$

Fourier transforming Eq. (4) with respect to  $y$  and  $z$ , we obtain

$$\sum_\sigma A_\sigma^{mn} \mathbf{e}_\sigma^{mn} = \frac{1}{ab} \int dy dz \mathbf{E}_\mathbf{T}(0, y, z) e^{-2\pi i(my/a + nz/b)} . \quad (6)$$

Since the  $\mathbf{e}_\sigma^{mn}$ ,  $\sigma = 1, 2$  are linearly independent, we can construct a set of adjoint eigenvectors  $\mathbf{e}_\sigma^{\dagger mn}$  such that

$$\mathbf{e}_\sigma^{\dagger mn} \cdot \mathbf{e}_{\sigma'}^{mn} = \delta_{\sigma\sigma'} . \quad (7)$$

For example, if one chooses for the magnetic field polarization vectors  $\mathbf{b}_{\sigma=1}^{mn} = (1, 0)$  and  $\mathbf{b}_{\sigma=2}^{mn} = (0, 1)$ , the adjoint eigenvectors are simply given by

$$\mathbf{e}_\sigma^{\dagger mn} = [\mathbf{Z}^{mn}]^{-1} \cdot \mathbf{e}_\sigma^{mn} .$$

Using these, Eq. (6) can be solved for the  $A_\sigma^{mn}$  to give

$$A_\sigma^{mn} = \frac{1}{ab} \int dy dz \mathbf{e}_\sigma^{\dagger mn} \cdot \mathbf{E}_\mathbf{T}(0, y, z) e^{-2\pi i(my/a + nz/b)} . \quad (8)$$

Substituting Eq. (8) in Eq. (5) gives

$$\begin{aligned} \mathbf{B}_{\mathbf{T}}(0, y, z) &= \sum_{m n \sigma} \mathbf{b}_{\sigma}^{m n} e^{2\pi i(m y/a + n z/b)} \\ &\times \frac{1}{ab} \int dy' dz' \mathbf{e}_{\sigma}^{\dagger m n} \cdot \mathbf{E}_{\mathbf{T}}(0, y', z') e^{-2\pi i(m y'/a + n z'/b)} \\ &= \int dy' dz' \mathbf{H}(y - y', z - z') \cdot \mathbf{E}_{\mathbf{T}}(0, y, z) , \end{aligned} \quad (9)$$

where the dyadic kernel  $\mathbf{H}(y - y', z - z')$  is given by

$$\mathbf{H}(y - y', z - z') = \sum_{m n \sigma} \mathbf{b}_{\sigma}^{m n} \mathbf{e}_{\sigma}^{\dagger m n} e^{2\pi i[m(y - y')/a + n(z - z')/b]} . \quad (10)$$

Equation (9) constitutes the desired condition, which enforces outgoing energy flux into the plasma. Since our interest here is to impose this boundary condition on a finite solution in the vacuum region, Eq. (9) must be discretized in some manner. Again, the precise way in which this is to be done depends on the details of implementation of the numerical finite solution, for example, on whether the solution is by finite differences or finite elements. For concreteness we consider a finite difference solution such that the field quantities are defined on a grid of mesh points  $(x_i, y_j, z_k)$ . The integral in Eq. (9) is obtained from a quadrature rule of the form

$$\mathbf{B}_{\mathbf{T}}(0, y_i, z_j) = \sum_{lm} \mathbf{W}_{ij;lm} \cdot \mathbf{E}_{\mathbf{T}}(0, y_l, z_m) , \quad (11)$$

where  $\mathbf{W}_{ij;lm}$  are the weights of the quadrature rule.

In the special but important case of grid points uniformly spaced in  $y$  and  $z$ , one can dispense with the integral quadrature altogether and represent the fields at the grid points directly in terms of discrete Fourier transforms. Denote the grid points on the plasma-vacuum boundary as  $y_i = ia/N_y$ ,  $0 \leq i \leq N_y$  and  $z_j = jb/N_z$ ,  $0 \leq j \leq N_z$ , where  $N_y$  and  $N_z$  are the number of grid points in each direction. Then Eq. (4) can be expressed as

$$\mathbf{E}_{\mathbf{T}}(0, y_i, z_j) = \sum_{m n \sigma} A_{\sigma}^{m n} \mathbf{e}_{\sigma}^{m n} e^{2\pi i(mi/N_y + nj/N_z)} \quad (4')$$

and similarly for Eq. (5). Taking a discrete Fourier transform of this equation gives

$$\sum_{\sigma} A_{\sigma}^{mn} e_{\sigma}^{mn} = \frac{1}{N_y N_z} \sum_{i=0, j=0}^{N_y, N_z} \mathbf{E}_{\mathbf{T}}(0, y_i, z_j) e^{-2\pi i(m i/N_y + n j/N_z)}, \quad (6')$$

$$-\frac{N_y}{2} \leq m \leq \frac{N_y}{2}, \quad -\frac{N_z}{2} \leq n \leq \frac{N_z}{2}.$$

From the Nyquist sampling theorem we know that  $N + 1$  sample points will serve to define  $N + 1$  Fourier harmonics, which we take in Eq. (6') to lie in the range  $-(N_y/2) \leq m \leq (N_y/2)$ ,  $-(N_z/2) \leq n \leq (N_z/2)$ . Equation (6') can be solved for the  $A_{\sigma}^{mn}$  using the adjoint eigenvectors, as Eq. (8) was. When these coefficients are used in the discrete Fourier representation for  $\mathbf{B}_{\mathbf{T}}(0, y, z)$ , one obtains an equivalent of Eq. (9),

$$\mathbf{B}_{\mathbf{T}}(0, y_i, z_j) = \sum_{l, k=0}^{N_y, N_z} \mathbf{H}(y_i - y'_l, z_j - z'_k) \cdot \mathbf{E}_{\mathbf{T}}(0, y_l, z_k), \quad (9')$$

where

$$\mathbf{H}(y_i - y'_l, z_j - z'_k) = \sum_{m=-\frac{N_y}{2}, n=-\frac{N_z}{2}, \sigma}^{\frac{N_y}{2}, \frac{N_z}{2}} \mathbf{B}_{\sigma}^{mn} e_{\sigma}^{\dagger mn} e^{i[m(i-l)/N_y + n(j-k)/N_z]}. \quad (10')$$

This is precisely what would be obtained from Eq. (11) in the case of equally spaced grid points where the quadrature formula is the simple trapezoidal rule with increments  $h_y = a/N_y$  and  $h_z = b/N_z$ . Then the weights  $\mathbf{W}_{ij;lm}$  are simply

$$\mathbf{W}_{ij;lm} = h_y h_z \mathbf{H}(y_i - y_l, z_j - z_m). \quad (12)$$

Equation (11) [or Eq. (9') for the case of a uniform grid] constitutes the desired discretized boundary condition on  $\mathbf{B}_{\mathbf{T}}$  in terms of the values of  $\mathbf{E}_{\mathbf{T}}$  evaluated at the grid points.

### 3. APPLICATION TO A SIMPLE 2D PROBLEM

#### 3.1. Reduction of the Boundary Condition to Fast Wave

##### *Propagation in Two Dimensions*

In order to verify that this scheme does indeed enforce the expected condition on energy flow, we have developed a finite difference solution of the simple 2D problem sketched in Fig. 2. The plasma region,  $x > 0$ , is again uniform in  $y$  and  $z$ . A sheet,  $y$ -directed current distribution is present at  $x = -x_A$ ,

$$\mathbf{J}_{\text{ext}}(x, z) = J_y(z) \delta(x + x_A) \hat{\mathbf{y}}, \quad (13)$$

and a flat conducting wall is located at  $x = -x_w$ . Further, we restrict consideration to the TE mode of propagation, or fast wave, for which  $\mathbf{E}(x, z) = E_y(x, z) \hat{\mathbf{y}}$  and  $\mathbf{B}(x, z) = B_x(x, z) \hat{\mathbf{x}} + B_z(x, z) \hat{\mathbf{z}}$ . In this case, it is convenient to eliminate  $\mathbf{B}$  using Faraday's law,

$$B_z = \frac{1}{i\omega} \frac{\partial E_y}{\partial x}, \quad B_x = \frac{-1}{i\omega} \frac{\partial E_y}{\partial z}. \quad (14)$$

We then work with the second-order equation for  $E_y$  alone,

$$\nabla^2 E_y + \frac{\omega^2}{c^2} E_y = -i\omega J_y, \quad (15)$$

where  $\nabla^2 = (\partial^2/\partial x^2) + (\partial^2/\partial z^2)$ .

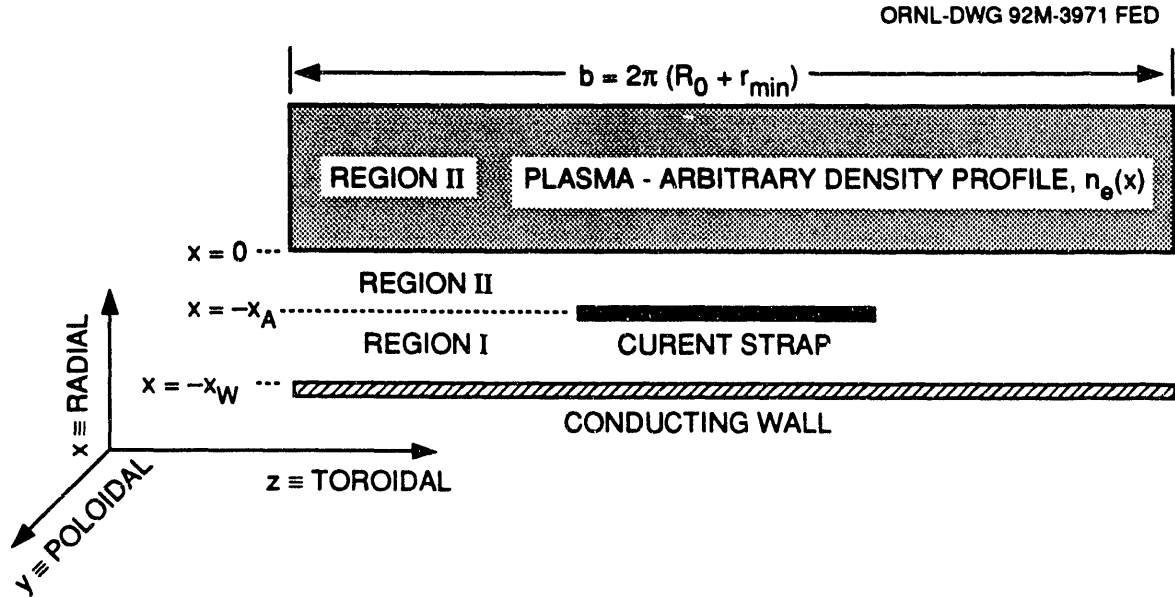


Fig. 2. Geometry for 2D problem.

In the plasma region we can write  $E_y(x, z)$  as

$$E_y(x, z) = \sum_n A_n E^n(x) e^{inKz} , \quad (16)$$

where  $K = 2\pi/b$ ,  $E^n(x)$  is the outgoing energy solution of the ordinary differential equation

$$\left[ \frac{\partial^2}{\partial x^2} + k_x^2(x, n) \right] E^n(x) = 0 , \quad (17)$$

and  $k_x^2(x, n)$  is the fast wave solution of the plasma dispersion relation  $D(\omega, x, k_x, k_z = nK) = 0$ .

For the finite difference solution of Eq. (15) we will require a boundary condition relating  $E'_y(x, z)$  [or equivalently  $B_z(x, z)$ ] to  $E_y(x, z)$ . Here the prime refers to differentiation by  $x$ . Differentiating Eq. (16) gives

$$E'_y(x, z) = \sum_n A_n E'^n(x) e^{inKz} ,$$

or, introducing the notation  $f_n \equiv E'^n(0)$  and  $e_n \equiv E^n(0)$ , we have

$$E_y(0, z) = \sum_n A_n e_n e^{inKz} , \quad E'_y(0, z) = \sum_n A_n f_n e^{inKz} . \quad (18)$$

Note that for this problem the plasma surface impedance matrix of Sect. 3 reduces to a scalar surface impedance  $Z^n = i\omega e_n / f_n$  such that  $E_y^n(0) = Z^n B_z^n(0)$ . We can solve for  $A_n$  in the first part of Eq. (18) by Fourier transformation,

$$A_n = \frac{1}{be_n} \int_0^b dz e^{-inKz} E_y(0, z) , \quad (19)$$

which, when used in the second part of Eq. (18), gives

$$\begin{aligned} E'_y(0, z) &= \sum_n \frac{f_n}{be_n} e^{inKz} \int_0^b dz' e^{-inKz'} E_y(0, z') \\ &= \int_0^b dz' H(z - z') E_y(0, z') , \end{aligned} \quad (20)$$

where the kernel  $H(z - z')$  is given by

$$H(z - z') = \sum_n \frac{f_n}{be_n} e^{inK(z-z')} . \quad (21)$$

Equation (20) is, of course, the reduction to this problem of the more general boundary condition expressed in Eq. (9). If the integral in Eq. (20) is performed using trapezoidal rule quadrature with increment  $h_z$ , the discretized version of Eq. (20) can be written

$$E'_y(0, z_i) = \sum_j h_z H(z_i - z_j) E_y(0, z_j) . \quad (22)$$

It is instructive to consider a case in which a single Fourier mode in  $z$  is present,  $J_y(z) = e^{inKz}$ . Then  $E_y(0, z_i) = E_0 e^{inKz_i}$  and Eq. (22) can be expressed as

$$\begin{aligned} E'_y(0, z_i) &= h_z E_0 \sum_{j=1}^{N_z} H(z_i - z_j) e^{inKz_j} = h_z E_0 \sum_{j=1}^{N_z} \sum_m \frac{f_m}{be_m} e^{imK(z_i - z_j)} e^{inKz_j} \\ &= \frac{h_z}{b} E_0 \sum_m \frac{f_m}{e_m} e^{imKz_i} \sum_{j=1}^{N_z} e^{2\pi i(j/N_z)(m-n)} . \end{aligned} \quad (23)$$

The second sum is a geometric series that can be evaluated to yield  $N_z \delta_{m-n, \nu N_z}$  for  $\nu = 0, \pm 1, \pm 2, \dots$ , so that Eq. (23) reduces to

$$E'_y(0, z_i) = E_0 \left[ \frac{f_n}{e_n} e^{inKz_i} + \frac{f_{n+N_z}}{e_{n+N_z}} e^{i(n+N_z)Kz_i} + \frac{f_{n-N_z}}{e_{n-N_z}} e^{i(n-N_z)Kz_i} + \dots \right] . \quad (24)$$

The correct value,  $E'_y(0, z_i) = E_0 f_n / e_n e^{inKz_i}$ , is obtained only if the sum over  $m$  in Eq. (23) is restricted to the range  $0 \leq |m| \leq N_z/2$  and  $n$  itself is restricted to  $0 \leq |n| \leq N_z/2 - 1$ . This is the expected result in consideration of the discussion following Eq. (6').

### 3.2. Implementation in a 2D Finite Difference Code

A finite difference solution of Eq. (15) is to be obtained in the vacuum region ( $-x_w \leq x \leq 0, 0 \leq z \leq b$ ) on the mesh  $x_i = -x_w + ih_z, z_j = jh_z$  for  $i = 0, N_x, j = 0, N_z$ , where  $h_x = x_w/N_x, h_z = b/N_z$ . Defining  $E_{i,j} \equiv E_y(x_i, z_j)$ , we can write the finite difference form of Eq. (15) as

$$\frac{1}{h_x^2} (E_{i+1,j} + E_{i-1,j}) + \frac{1}{h_z^2} (E_{i,j+1} + E_{i,j-1}) + \left[ \frac{\omega^2}{c^2} - 2 \left( \frac{1}{h_x^2} + \frac{1}{h_z^2} \right) \right] E_{i,j} = \frac{-i\omega}{h_x} J_{i,j} . \quad (25)$$

Imposing perfect conductivity on the wall gives  $E_{0,j} = 0$ . Periodicity at  $z = 0, b$  gives  $E_{i,0} = E_{i,N_z}$ . And continuity of  $\partial E_y / \partial z$  at  $z = 0, b$  gives  $E_{i,N_z+1} = E_{i,1}, E_{i,0-1} = E_{i,N_z-1}$ . At the plasma-vacuum boundary,  $i = N_z$ , Eq. (25) requires  $E_{N_z+1,j}$ , which is obtained from the finite difference representation of  $E'_y$ ,

$$E'_y(0, z_j) = \frac{1}{2h_x} (E_{N_z+1,j} - E_{N_z-1,j}) .$$

Using Eq. (22) and solving for  $E_{N_z+1,j}$  gives

$$E_{N_z+1,j} = E_{N_z-1,j} + 2h_x h_z \sum_j H_{i,j} E_{N_z,j} , \quad (26)$$

where

$$H_{i,j} = \sum_{m=-N_z/2}^{N_z/2} \frac{f_m}{b\varepsilon_m} \exp \left[ 2\pi i \left( \frac{m}{N_z} \right) (i - j) \right] . \quad (27)$$

Equation (25), with the associated boundary conditions discussed above, constitutes a linear system for  $E_{i,j}$  which is solved using a standard matrix inversion package.

#### 4. RESULTS OF 2D CALCULATION AND DISCUSSION

The problem sketched in Fig. 2 is 2D only because of the  $z$ -dependence of the antenna current, the inhomogeneous term of Eq. (15). As a result the problem can easily be solved by Fourier transformation in the  $z$ -direction. In the plasma region, the field is again given by an expansion of the form of Eq. (16). In the two vacuum regions, region I =  $(-x_w \leq x < -x_A)$ , region II =  $(-x_A \leq x \leq 0)$ , the expansion is of the form

$$E_y^{I,II}(x, z) = \sum_n C_n^+ e^{i(+\kappa_n x + nKz)} + C_n^- e^{i(-\kappa_n x + nKz)} ,$$

where  $\kappa_n$  is the wave number obtained from the vacuum dispersion relation  $(\omega^2/c^2) = \kappa_n^2 + n^2 K^2$ . Imposing the conditions of vanishing  $E_y$  at  $x = -x_w$ , continuity of the field and its derivative at the plasma-vacuum boundary, and the jump condition  $E'_y(-x_{A+}) - E'_y(-x_{A-}) = -\omega J_y$  at the strap location, one can

eliminate the unknown coefficients  $C_n^\pm, A_n$  and obtain a complete solution. In particular, the expansion coefficients  $A_n$  in Eq. (16) are given by

$$A_n = -\omega\mu_0 J_n \frac{\sin[\kappa_n(x_w - x_A)]}{f_n/b_n \sin(\kappa_n x_w) + i\kappa_n \cos(\kappa_n x_w)}, \quad (28)$$

where  $J_n$  is the  $n$ th Fourier component of  $J_y(z)$ .

To compare the two computations we have plotted the field at the plasma boundary  $E_y(0, z)$  versus  $z$  as obtained by the Fourier method of Eq. (28), Fig. 3a, and by the 2D finite difference method, Fig. 3b. The plasma parameters are representative of a modest-size tokamak:  $n_e(0) = 4.5 \times 10^{19} \text{ cm}^{-3}$  with a parabolic profile,  $n_e(x) = n_e(0)(1 - x^2/a^2)$ ,  $a = 60 \text{ cm}$ ,  $B_0 = 2 \text{ T}$ . The cold plasma conductivity was used. The geometric parameters were chosen for convenience of comparison of the two calculations:  $b = 1000 \text{ cm}$ ,  $x_A = 5 \text{ cm}$ ,  $x_w = 15 \text{ cm}$ . The strap current distribution is constant, with a width of 200 cm, and is centered in the domain, at  $z = 500 \text{ cm}$ . The RF frequency is  $f_{\text{RF}} = 125 \text{ MHz}$ . Figure 3a was calculated with 150 Fourier modes. One can see that the field is small except in front of the current strap and that there are oscillations at the ends of the strap due to Gibbs phenomena. The solid curves are  $\text{Re}\{E_y(0, z)\}$ , and the dashed curves are  $\text{Im}\{E_y(0, z)\}$ . Figure 3b was calculated with 30 grid points in each dimension. The discrete nature of

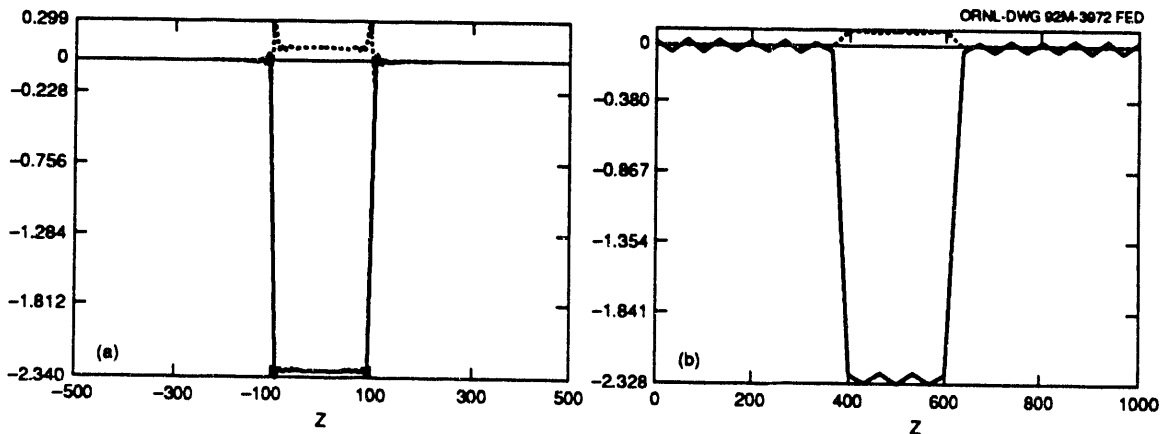


Fig. 3. Electric field at the plasma-vacuum boundary,  $\text{Re}E_y(0, z)$  (solid curves) and  $\text{Im}E_y(0, z)$  (dashed curves), obtained from (a) the Fourier solution and (b) the finite difference solution.

the solution is evident. The important point is that the field amplitudes agree to within about 1%. The Poynting flux at the first grid point inside the vacuum region obtained from the finite difference solution is shown in Fig. 4. We see that the small-amplitude oscillations appearing in Fig. 3b away from the antenna do not result in a nonphysical power flow there. Another important comparison is the total radiated power in the two models. Summing the power radiated into each mode of the Fourier solution yields  $P_{\text{tot}} = 0.754 \text{ W}\cdot\text{A}^{-1}\cdot\text{m}^{-1}$ . Integrating the real part of  $\mathbf{E} \cdot \mathbf{J}$  along the current strap for the finite difference case gives  $P_{\text{tot}} = 0.736 \text{ W}\cdot\text{A}^{-1}\cdot\text{m}^{-1}$ , an agreement of 2%. We conclude therefore that the boundary condition proposed above does indeed yield a well-conditioned linear system and does enforce the proper energy flux on the finite difference solution.

Figure 5 shows a plot of the kernel function of Eq. (27),  $H_{i,0}$ , which is a measure of the coupling between points on the boundary with spacing  $\Delta x = ih_z$ . The function is purely imaginary and highly peaked at  $i = 0$ . This strong coupling of each boundary point to itself and the lack of much interesting structure in  $H_{i,0}$  away from  $i = 0$  cause one to wonder whether the coupling is in some sense trivial and whether the structure of  $H_{i,j}$  is really significant. To

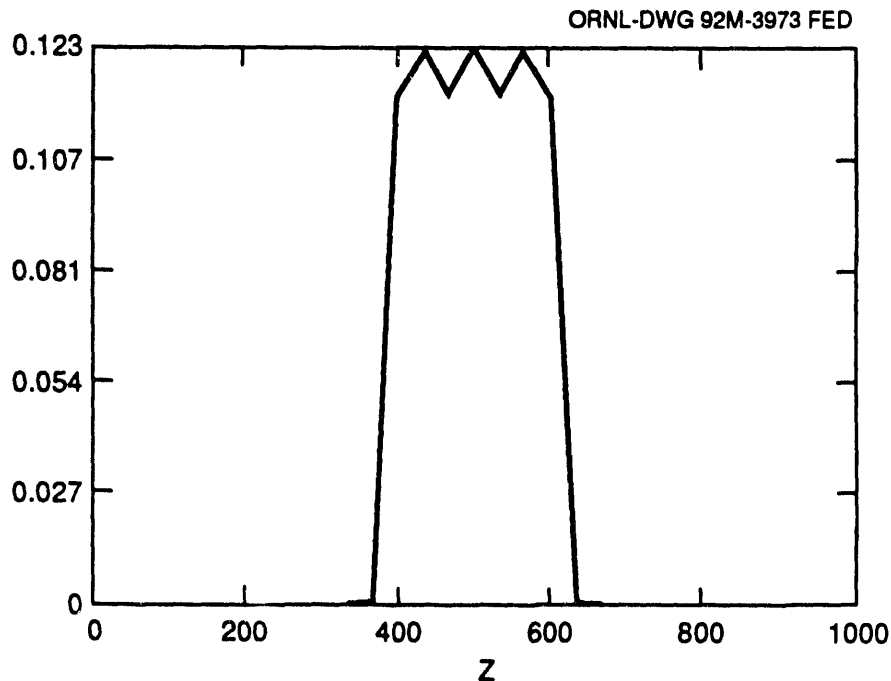


Fig. 4. Poynting flux  $S_z$  versus  $z$  for the finite difference solution (Fig. 3a).

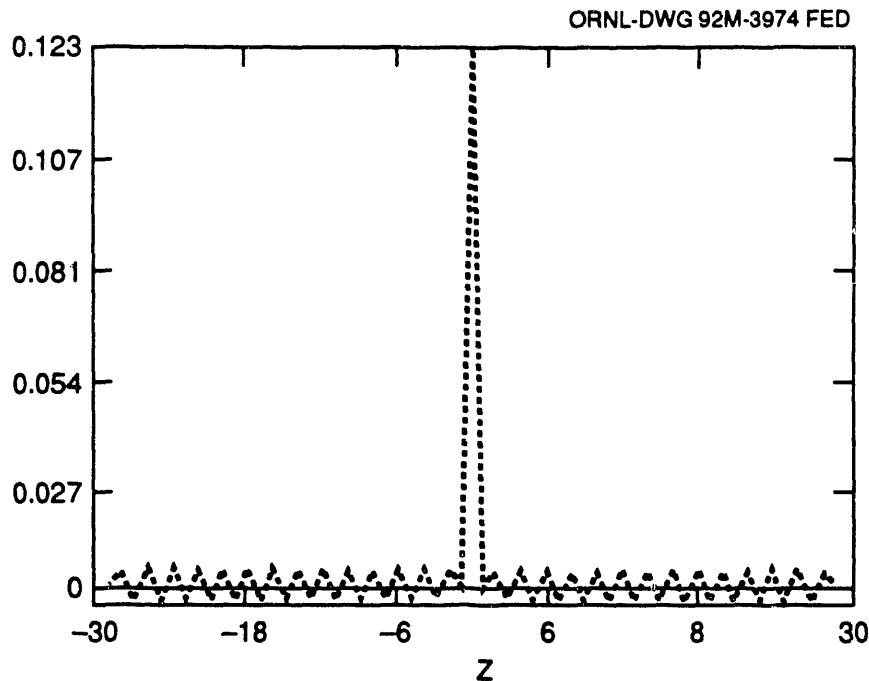


Fig. 5. Kernel function  $H_{i,0}$  versus point spacing,  $i$  as calculated for Eq. (27) using the correct number of Fourier modes,  $-N_z/2 \leq n \leq N_z/2$ .

investigate this, we have run the same case as shown in Fig. 3 but with the sum in Eq. (27) extending over different ranges of  $m$ . Figure 6a shows  $H_{i,0}$  calculated taking one less term at each end of the sum range,  $-(N_z/2 - 1) \leq n \leq (N_z/2 - 1)$ . The difference between this and Fig. 5 is rather subtle; however, the effect on the solution, shown in Fig. 6b, is striking compared to Fig. 3b. In this case the imaginary part of the solution is completely unstable, and the calculated power is  $P_{\text{tot}} = 1.67 \text{ W} \cdot \text{A}^{-1} \cdot \text{m}$ , a factor of 2.2 error. Taking an additional term in the sum over  $m$  has a smaller but still significant effect.

We anticipate extending this calculation to three dimensions and including all three electric field components. To do this, some computational issues must be resolved. The matrix structure is block-tridiagonal except for the equations connecting to the plasma boundary points, which are dense. Clearly it will not be feasible to solve the complete system arising from the 3D problem as a dense matrix. Since the coupling to non-nearest-neighbor points through the kernel is weak, one could imagine solving the uncoupled problem using sparse matrix techniques, then solving with coupling by iteration. In any case, there are opportunities here for creative linear algebra.

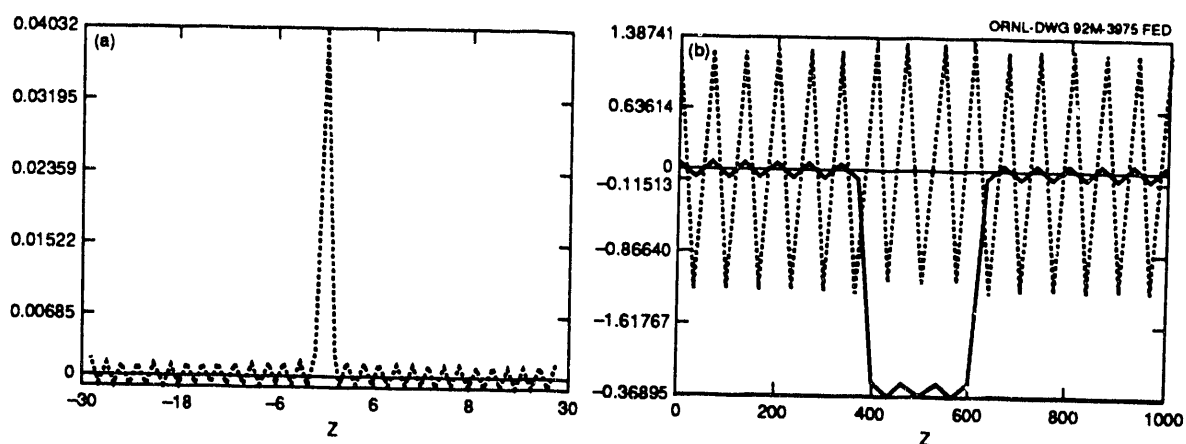


Fig. 6. (a) Kernel function  $H_{i,0}$  versus point spacing,  $i$  as calculated for Eq. (27) using fewer Fourier modes,  $-(N_z/2 - 1) \leq n \leq (N_z/2 - 1)$ . (b) Electric field at the plasma-vacuum boundary,  $\text{Re}E_y(0, z)$  (solid curves) and  $\text{Im}E_y(0, z)$  (dashed curves), obtained from the finite difference solution using the kernel shown in (a).

### ACKNOWLEDGMENT

The authors thank D. C. Stallings, E. F. Jaeger, and Y. L. Ho for useful discussions.

**REFERENCES**

KRESS M., HO Y. L., GROSSMAN W., DOBROTT A., BATCHELOR D. B., RYAN P. M., and CARTER M. D. (1992) AIP Conf. Proc. 244, 213.

RYAN P. M., ROTHE K. E., WHEALTON J. H., and SHEPARD T. D. (1990) *Fusion Eng. Des.* 12, 37.

BATCHELOR D. B., CARTER M. D., GOLDFINGER R. C., STALLINGS D. C., and TOLLIVER J. S. (1992) unpublished.

**INTERNAL DISTRIBUTION**

- |   |                        |
|---|------------------------|
| 1. Director, ORNL Fusion Energy Division  | 21. ORNL Patent Office |
| 2. C. C. Baker                            | 22-26. D. B. Batchelor |
| 3. M. J. Saltmarsh                        | 27-31. M. D. Carter    |
| 4. L. A. Berry                            | 32. F. W. Baity        |
| 5. B. A. Carreras                         | 33. T. S. Bigelow      |
| 6. R. A. Dory                             | 34. R. C. Goldfinger   |
| 7. J. L. Dunlap                           | 35. R. H. Goulding     |
| 8. H. H. Haselton                         | 36. S. P. Hirshman     |
| 9. M. S. Lubell                           | 37. D. J. Hoffman      |
| 10. T. E. Shannon                         | 38. W. A. Houlberg     |
| 11. R. P. Leinius                         | 39. E. F. Jaeger       |
| 12-13. Laboratory Records Department      | 40. D. A. Rasmussen    |
| 14. Laboratory Records, ORNL-RC           | 41. P. M. Ryan         |
| 15-16. Central Research Library           | 42. D. C. Stallings    |
| 17. Document Reference Section            | 43. D. W. Swain        |
| 18. Fusion Energy Division Library        | 44. J. H. Whealton     |
| 19-20. ET/FE Division Publications Office | 45. J. J. Yugo         |

**EXTERNAL DISTRIBUTION**

46. Office of the Assistant Manager for Energy Research and Development, U.S. Department of Energy Field Office, Oak Ridge, P.O. Box 2000, Oak Ridge, TN 37831
47. N. A. Davies, Director, Office of Fusion Energy, Office of Energy Research, ER-50 Germantown, U.S. Department of Energy, Washington, DC 20545
48. M. Roberts, International Programs, Office of Fusion Energy, Office of Energy Research, ER-52 Germantown, U.S. Department of Energy, Washington, DC 20545
49. D. E. Baldwin, Lawrence Livermore National Laboratory, P.O. Box 5511, Livermore, CA 94550
50. R. W. Conn, Mechanical, Aerospace, and Nuclear Engineering Department, 6291 Boelter Hall, University of California, Los Angeles, CA 90024-1597
51. P. C. Liewer, MS 138-208, Jet Propulsion Laboratory, 4800 Oak Grove Drive, Pasadena, CA 91109
52. D. Sigmar, Plasma Fusion Center, Massachusetts Institute of Technology, 167 Albany St., NW16-288, Cambridge, MA 02139
53. K. I. Thomassen, L-637, Lawrence Livermore National Laboratory, P.O. Box 5511, Livermore, CA 94550
54. J. D. Callen, Department of Nuclear Engineering, University of Wisconsin, Madison, WI 53706-1687
55. S. O. Dean, Fusion Power Associates, Inc., 2 Professional Drive, Suite 248, Gaithersburg, MD 20879
56. H. K. Forsen, Bechtel Group, Inc., Research Engineering, P.O. Box 3965, San Francisco, CA 94119
57. R. W. Gould, Department of Applied Physics, California Institute of Technology, Pasadena, CA 91125

58. R. A. Gross, Plasma Research Laboratory, Columbia University, New York, NY 10027
59. R. J. Hawryluk, Plasma Physics Laboratory, Princeton University, P.O. Box 451, Princeton, NJ 08543
60. D. M. Meade, Plasma Physics Laboratory, Princeton University, P.O. Box 451, Princeton, NJ 08543
61. W. M. Stacey, School of Nuclear Engineering and Health Physics, Georgia Institute of Technology, Atlanta, GA 30332
62. D. Steiner, Nuclear Engineering Department, NES Building, Tibbetts Avenue, Rensselaer Polytechnic Institute, Troy, NY 12181
63. R. Varma, Physical Research Laboratory, Navrangpura, Ahmedabad 380009, India
64. Bibliothek, Max-Planck Institut für Plasmaphysik, Boltzmannstrasse 2, D-8046 Garching, Federal Republic of Germany
65. Bibliothek, Institut für Plasmaphysik, KFA Jülich GmbH, Postfach 1913, D-5170 Jülich, Federal Republic of Germany
66. Bibliothek, KfK Karlsruhe GmbH, Postfach 3640, D-7500 Karlsruhe 1, Federal Republic of Germany
67. Bibliotheque, Centre de Recherches en Physique des Plasmas, Ecole Polytechnique Fédérale de Lausanne, 21 Avenue des Bains, CH-1007 Lausanne, Switzerland
68. R. Aymar, CEN/Cadarache, Département de Recherches sur la Fusion Contrôlée, F-13108 Saint-Paul-lez-Durance Cedex, France
69. Bibliothèque, CEN/Cadarache, F-13108 Saint-Paul-lez-Durance Cedex, France
70. Library, JET Joint Undertaking, Abingdon, Oxfordshire OX14 3EA, England
71. Library, FOM-Instituut voor Plasmafysica, Rijnhuizen, Edisonbaan 14, 3439 MN Nieuwegein, The Netherlands
72. Library, National Institute for Fusion Science, Chikusa-ku, Nagoya 464-01, Japan
73. Library, International Centre for Theoretical Physics, P.O. Box 586, I-34100 Trieste, Italy
74. Library, Centro Ricerca Energia Frascati, C.P. 65, I-00044 Frascati (Roma), Italy
75. Library, Plasma Physics Laboratory, Kyoto University, Gokasho, Uji, Kyoto 611, Japan
76. Plasma Research Laboratory, Australian National University, P.O. Box 4, Canberra, A.C.T. 2601, Australia
77. Library, Japan Atomic Energy Research Institute, Naka Fusion Research Establishment, 801-1 Mukoyama, Naka-machi, Naka-gun, Ibaraki-ken, Japan
78. G. A. Eliseev, I. V. Kurchatov Institute of Atomic Energy, P.O. Box 3402, 123182 Moscow, Russia
79. V. A. Glukhikh, Scientific-Research Institute of Electro-Physical Apparatus, 188631 St. Petersburg, Russia
80. I. Shpigel, Institute of General Physics, U.S.S.R. Academy of Sciences, Ulitsa Vavilova 38, Moscow, Russia
81. D. D. Ryutov, Institute of Nuclear Physics, Siberian Academy of Sciences, Sovetskaya St. 5, 630090 Novosibirsk, Russia
82. O. Pavlichenko, Kharkov Physical-Technical Institute, Academical St. 1, 310108 Kharkov, Ukraine
83. Deputy Director, Southwestern Institute of Physics, P.O. Box 15, Leshan, Sichuan, China (PRC)
84. Director, The Institute of Plasma Physics, P.O. Box 1126, Hefei, Anhui, China (PRC)
85. R. H. McKnight, Experimental Plasma Research Branch, Division of Development and Technology, Office of Fusion Energy, Office of Energy Research, ER-542 Germantown, U.S. Department of Energy, Washington, DC 20545

86. D. Crandall, Director, Division of Applied Plasma Physics, Office of Fusion Energy, Office of Energy Research, ER-54 Germantown, U.S. Department of Energy, Washington, DC 20545
87. E. Oktay, Division of Confinement Systems, Office of Fusion Energy, Office of Energy Research, ER-55 Germantown, U.S. Department of Energy, Washington, DC 20545
88. W. Sadowski, Fusion Theory and Computer Services Branch, Division of Applied Plasma Physics, Office of Fusion Energy, Office of Energy Research, ER-541 Germantown, U.S. Department of Energy, Washington, DC 20545
89. R. E. Mickens, Atlanta University, Department of Physics, Atlanta, GA 30314
90. M. N. Rosenbluth, University of California at San Diego, La Jolla, CA 92037
91. D. Schnack, SAIC, 10260 Campus Point Drive, San Diego, CA 92121
92. Duk-In Choi, Department of Physics, Korea Advanced Institute of Science and Technology, P.O. Box 150, Chong Ryang-Ri, Seoul, Korea
93. Library of Physics Department, University of Ioannina, Ioannina, Greece
94. C. De Palo, Library, Associazione EURATOM-ENEA sulla Fusione, CP 65, I-00044 Frascati (Roma), Italy
95. Laboratorio Associado de Plasma, Instituto Nacional de Pesquisas Espaciais, Caixa Postal 515, 122201, Sao Jose dos Campos, SP, Brazil
96. Theory Department Read File, c/o D. W. Ross, University of Texas, Institute for Fusion Studies, Austin, TX 78712
97. Theory Department Read File, c/o R. Parker, Director, Plasma Fusion Center, NW 16-202, Massachusetts Institute of Technology, Cambridge, MA 02139
98. Theory Department Read File, c/o R. White, Plasma Physics Laboratory, Princeton University, P.O. Box 451, Princeton, NJ 08543
99. Theory Department Read File, c/o L. Kovrizhnykh, Lebedev Institute of Physics, Academy of Sciences, 53 Leninsky Prospect, 117924 Moscow, Russia
100. Theory Department Read File, c/o B. B. Kadomtsev, I. V. Kurchatov Institute of Atomic Energy, P.O. Box 3402, 123182 Moscow, Russia
101. Theory Department Read File, c/o T. Kamimura, National Institute for Fusion Studies, Nagoya 464, Japan
102. Theory Department Read File, c/o E. Maschke, Departemente de Recherches sur la Fusion Controlée, CEN/Cadarache, F-13108 Saint-Paul-lez Durance, France
103. Theory Department Read File, c/o D. Düchs, JET Joint Undertaking, Abingdon, Oxfordshire OX14 3EA, United Kingdom
104. Theory Department Read File, c/o R. Briscoe, Culham Laboratory, Abingdon, Oxfordshire OX14 3DB, United Kingdom
105. Theory Department Read File, c/o D. Biskamp, Max-Planck-Institut für Plasmaphysik, Boltzmannstrasse 2, D-8046 Garching, Federal Republic of Germany
106. Theory Department Read File, c/o T. Takeda, Japan Atomic Energy Research Institute, Tokai Fusion Research Establishment, Tokai-mura, Naka-gun, Ibaraki-ken, Japan
107. Theory Department Read File, c/o J. Greene, General Atomics, P.O. Box 85608, San Diego, CA 92186
108. Theory Department Read File, c/o R. Cohen, Lawrence Livermore National Laboratory, P.O. Box 5511, Livermore, CA 94550
109. Theory Department Read File, c/o R. Gerwin, CTR Division, Los Alamos National Laboratory, P.O. Box 1663, Los Alamos, NM 87545
110. R. Aamodt, Lodestar Research Corporation, 2400 Central Avenue, Boulder, CO 80301
111. K. Appert, Centre de Recherches en Physique des Plasmas, Ecole Polytechnique Fédérale de Lausanne, 21 Avenue des Bains, CH-1007 Lausanne, Switzerland

112. M. Ballico, Max-Planck Institut für Plasmaphysik, Boltzmannstrasse 2, D-8046 Garching, Federal Republic of Germany
113. E. Barbato, Associazione EURATOM-ENEA sulla Fusione, Centro Recherche Energia Frascati, C.P. 65, I-00044 Frascati (Roma), Italy
114. A. Bécoulet, Association EURATOM-CEA sur la Fusion Controlée, Centre d'Etudes Nucléaires de Cadarache, B. P. No. 1, F-13108 Saint Paul lez Durances, France
115. S. Bernabei, Plasma Physics Laboratory, Princeton University, P.O. Box 451, Princeton, NJ 08543
116. A. Bers, Plasma Fusion Center, Massachusetts Institute of Technology, 38-260, Cambridge, MA 02139
117. V. Bhatnagar, JET Joint Undertaking, Abingdon, Oxfordshire OX14 3EA, England
118. P. T. Bonoli, Plasma Fusion Center, Massachusetts Institute of Technology, 175 Albany St., NW17-115, Cambridge, MA 02139
119. M. Brambilla, Max-Planck Institut für Plasmaphysik, Boltzmannstrasse 2, D-8046 Garching, Federal Republic of Germany
120. Dr. Vincent Chan, General Atomics, P. O. Box 85608, San Diego, CA 92186
121. D. Ehst, Building 205, Argonne National Laboratory, 9700 S. Cass Avenue, Argonne, IL 60538
122. D. Faulconer, Laboratoire de Physique des Plasmas, EURATOM-Etat Belge, Ecole Royale Militaire, Avenue de la Renaissance 30, 1040 Brussels, Belgium
123. D. J. Gambier, JET Joint Undertaking, Abingdon, Oxfordshire OX14 3EA, England
124. S. N. Golovato, Plasma Fusion Center, Massachusetts Institute of Technology, 175 Albany Street, NW17-113, Cambridge, MA 02139
125. W. Grossman, SAIC, 1710 Goodridge Drive, McLean, VA 22102
126. W. Ho, SAIC, 10260 Campus Point Drive, San Diego, CA 92121
127. J. Hosea, Plasma Physics Laboratory, Princeton University, P.O. Box 451, Princeton, NJ 08543
128. Kwok Ko, Stanford Linear Accelerator Center, P.O. Box 4349, Stanford, CA 94309
129. C. C. Petty, General Atomics, P.O. Box 85608, San Diego, CA 92186
130. C. K. Phillips, Plasma Physics Laboratory, Princeton University, P.O. Box 451, Princeton, NJ 08543
131. M. Porkolab, Plasma Fusion Center, Massachusetts Institute of Technology, 175 Albany Street, NW17-119, Cambridge, MA 02139
132. R. Prater, General Atomics, P.O. Box 85608, San Diego, CA 92186
133. J. Scharer, Electrical and Computer Engineering Department, 1500 Johnson Drive, University of Wisconsin, Madison, WI 53706
134. D. C. Stevens, Courant Institute for Mathematical Sciences, New York University, 251 Mercer Street, New York, NY 10001
135. P. E. Vandenplas, Laboratoire de Physique des Plasmas, EURATOM-Etat Belge, Ecole Royale Militaire, Avenue de la Renaissance 30, 1040 Brussels, Belgium
136. H. Weitzner, Courant Institute for Mathematical Sciences, New York University, 251 Mercer Street, New York, NY 10001
137. J. R. Wilson, Plasma Physics Laboratory, Princeton University, P.O. Box 451, Princeton, NJ 08543
- 138-85. Given distribution according to OSTI-4500, Magnetic Fusion Energy (Category Distribution UC-427, Theoretical Plasma Physics)

**END**

**DATE  
FILMED**

3 / 26 / 93

